Operating and Extreme weather conditions at Marine Renewable Energy Lab (MaRELab)

Contestabile, P., Russo, S., Azzellino, A., Cascetta, F. and Vicinanza, D.

Abstract—**The co-location of offshore wind turbines and wave energy converters has gained significant interest due to studies demonstrating the benefits of combined power production. When wind and wave technologies work together, the resulting power output is more predictable, less fluctuating, and offers greater continuity compared to their individual operation. However, the impact of thermal winds on nearshore locations, specifically concerning the combination of wind and wave resources, remains poorly understood. This study aims to address this knowledge gap by evaluating the effects of local sea winds and land breeze circulations on wave-wind resources. The researchers propose a methodology to estimate the viability of co-exploitation using various multivariate techniques. The case study focuses on the Marine Renewable Energy Laboratory in Italy and utilizes a comprehensive 42-year hindcast dataset. The researchers identify specific meteo-climatic conditions that favour the optimal combination of wind and wave sources in nearshore areas that represent a particularly attractive opportunity for maximizing power generation and minimizing fluctuations.**

Keywords— **Combined wave and wind energy, Blue energy management, Offshore wind, Nearshore wave energy, Mediterranean Sea meteorology.**

The present work is part of the "Ricerca di Sistema" project (RSE – PTR, 1.8 "Energia elettrica dal mare"), funded by Italian Ministry of Economic Development (MISE).

P. Contestabile is with Department of Engineering, University of Campania "Luigi Vanvitelli," Aversa, Italy (pasquale.contestabile@unicampania.it).

S. Russo is with Department of Engineering, University of Campania "Luigi Vanvitelli," Aversa, Italy (sar.russo@unicampania.it).

A. Azzellino is with the Civil and Environmental Engineering Department of the Politecnico di Milano, Milan, Italy (e-mail: arianna.azzellino@polimi.it).

F. Cascetta is with Department of Engineering, University of Campania "Luigi Vanvitelli," Aversa, Italy (pasquale.contestabile@unicampania.it).

D. Vicinanza is with Inter-University National Consortium for Marine Sciences (CoNISMa), P.zzale Flaminio, 00144 Rome, Italy (e-mail: vicinanza@conisma.it) and with Department of Engineering, University of Campania "Luigi Vanvitelli," Aversa, Italy (e-mail: diego.vicinanza@unicampania.it).

Digital Object Identifier: https://doi.org/10.36688/ewtec-2023-558

I. INTRODUCTION

Unlocking the potential of the offshore market in the Mediterranean is key to accelerating the long-term development of Offshore Renewables (ORs). The unique wind and wave conditions in this region differ from those in the North Sea and the Atlantic Ocean. These milder climatic conditions not only allow for more affordable infrastructure and device structures but also drive the need for site-specific technologies.

In addition to offshore solutions, the development of nearshore wind and wave energy offers a cost-reducing option that can bridge the gap between onshore and offshore development. This approach also benefits port authorities and coastal cities by promoting innovation, such as the creation of green ports [1,2,3], electrification of docks with clean energies [4,5,6], and renewable energy-based water desalination [7].

Studies have explored the potential of co-locating offshore wind turbines and wave energy converters, such as in the Danish portion of the North Sea, using Marine Spatial Planning [8,9]. These studies enable early identification of potential conflicts, such as ship traffic and fisheries, and support optimal siting of wind-wave parks for environmental sustainability [10]. The combined option of wind and wave energy presents advantages in terms of reduced environmental impact compared to standalone options [11,12].

The optimization of site selection for stand-alone energy devices may not be ideal when compared to the combined option, primarily due to the interplay of local wind and wave energy patterns. Along coastlines, a common occurrence is the sea and land breeze circulation, which is driven by differential heating of the water and nearby land surfaces [13]. The slower heating of water causes the air over the land to be warmer, resulting in higher surface pressure over the water and lower pressure over the land. This pressure difference leads to the sea breeze, where wind flows from the water to the land. At night, the land cools faster, creating a zone of higher pressure and generating the land breeze, with wind flowing from land to water.

In recent years, several authors have explored the combined utilization of offshore wind and wave energy resources. Numerous papers have examined both resources in parallel, albeit with a large-scale approach or

without considering the influence of thermal wind patterns accurately [e.g. 14,15]. Other studies have concentrated on assessing the nearshore impact of hybrid wave-wind energy farms in terms of hydrodynamic changes [e.g. 16,17]

To the best of our knowledge, our study represents one of the initial investigations into the simultaneous exploitation of energy from winds and waves in a nearshore setting.

The objective of this paper is to examine the impact of local meteorological patterns, specifically influenced by nearshore conditions, on wave and wind resources. The study proposes a methodology for assessing the complementarity, combination, and misalignment of co-developing wind-wave projects in nearshore locations.

Through a case study conducted at the innovative Marine Renewable Energy Laboratory (MaRELab) in Italy, this research illustrates a method that offers insights into evaluating the effectiveness of co-exploitation using various multivariate techniques. Importantly, this approach is applicable regardless of the specific wind and wave technologies employed at the site.

II. METHODS

A. *Study area*

MaRELab is situated in the Gulf of Naples, Italy, within the Middle Tyrrhenian Sea (Fig. 1). Its geographic coordinates are 40°49'58.68'' N and 14°16'03.64'' E, located in the middle of the San Vincenzo breakwater. This field laboratory is the result of a collaboration between the Institute of Marine Engineering of the National Research Council (INM-CNR) and the Department of Engineering of the University of Campania "Luigi Vanvitelli." The partnership aims to combine expertise in various aspects of "blue" engineering, drawing from experience in environmental, coastal, and naval fields. MaRELab represents a natural progression from the facilities established in 2015 to accommodate the OBREC (Overtopping Breakwater for wave Energy Conversion) prototype (Fig. 2) [18,19].

The selection of this site was based on logistical considerations, given its proximity to the city and Naples's harbour, as well as environmental factors. The calm sea states are prevalent during the summer season, and the wave climate exhibits a narrow directional sector. The 25-meter water depth at the breakwater's toe prevents breaking conditions, even during the period from November to March, when extreme waves occur [20]. These characteristics are advantageous for field monitoring requirements of both wind and wave energy devices. Successful monitoring activities necessitate calm conditions for safe installation and instrument maintenance [21]. From April to October, the wave climate has proven optimal for investigating 1:7 scale floating prototypes compared to conditions in the far offshore Tyrrhenian Sea [22]. In fact, during the summer and autumn of 2021, MaRELab hosted an innovative 1:10 scaled Floating Wind Prototype (Fig. 3). The primary objective of MaRELab is to demonstrate medium to full-scale marine energy systems in relevant operational environments. This field laboratory is particularly valuable for evaluating the energetic and structural performance of innovative devices, considering that the local "Mediterranean" meteo-climatic conditions differ significantly from those typically encountered in oceans or northern seas.

Fig. 1. The map illustrates the positioning of MaRELab, in Italy, in the Naples Gulf and at S. Vincenzo breakwater in the Port of Naples.

Fig. 2. Overtopping Breakwater for wave Energy Conversion prototype

Fig. 3. MaRELab sea view

B. *Wind and wave data*

This study utilized the ERA5 climate reanalysis dataset from the European Centre for Medium-Range Weather Forecasts (ECMWF) [23]. ERA5 provides hourly estimates of climate variables, superseding the previous ERA-Interim dataset. The ERA5 dataset covers the period from January 1979 to 5 days of real-time data. It offers increased time resolution, resulting in improved accuracy compared to ERA-Interim. The variables analyzed in this

study include peak wave period (Tp), mean wave direction, significant height of combined wind waves and swell (Hs), and 10m wind components (u and w).

The significant height of combined wind waves and swell, Hs, represents the average height of the highest one-third of surface sea waves generated by wind and swell. It is calculated as four times the square root of the integral over all directions and frequencies of the two-dimensional wave spectrum. Hs is a crucial parameter for assessing sea state and swell. The mean wave period, Tm, and mean wave direction, Dm, also consider both wind-sea waves influenced by local winds and swell generated elsewhere and at different times.

The 10m-u (and 10m-w) parameter represents the eastward (northward) component of the 10m wind, indicating the horizontal speed of air moving towards the east (north) at a height of ten meters above the Earth's surface, measured in meters per second. These parameters are combined to determine the speed and direction of the horizontal 10m wind, V10. Since wind data and wave parameters come from different sources, they are not provided at the same virtual grid points. The closest ECMWF point for wind (W1) with coordinates 40.83°N, 14.27°E is in close proximity to the laboratory facilities and can be used directly with minimal processing.

However, the ECMWF internal WAve Model (WAM) covers the Mediterranean Sea using a base model grid with a resolution of 0.75° x 0.75°. Therefore, the point P1 with coordinates 40.5°N, 14.0°E is located too far from the study site. To account for the complex variations in wave parameters from offshore the Gulf of Naples to the San Vincenzo's berth, the nearshore energetic patterns have been analysed.

C. *Wind power*

The total amount of kinetic energy flowing through an area R during the time t is expressed as:

$$E_{wind} = \frac{1}{2}\rho_a t R U_{10}^3 \tag{1}$$

where ϱ_a is the air density and U_{10} is the wind speed computed from the horizontal North-East wind components.

The electric power collected at the terminals is given by the following relation:

$$P_{wind} = \frac{1}{2}C_p(V)\rho_a R_b U_{10}^3 \tag{2}$$

where C_P (V) is the power coefficient and R_b represents the area swept by the rotating blades. The maximum theoretical value of C_P is 0.593. The maximum energy derived from a wind turbine is only the 59% of the available wind kinetic energy.

D. *Wave power*

The nearshore energetic patterns were analysed using the MIKE 21 SW spectral wave model, developed by DHI Water and Environment [24]. This numerical model incorporates factors such as refraction, shoaling, local wind generation, energy dissipation from bottom friction, and wave-breaking. The model's description has been previously outlined by Contestabile et al. [25]. The seabed information was obtained by interpolating data from the General Bathymetric Chart of the Oceans (GEBCO) database [26]. The computational domain was discretized using an unstructured grid with linear triangular elements, employing the cell-centred finite volume method (Fig. 4).

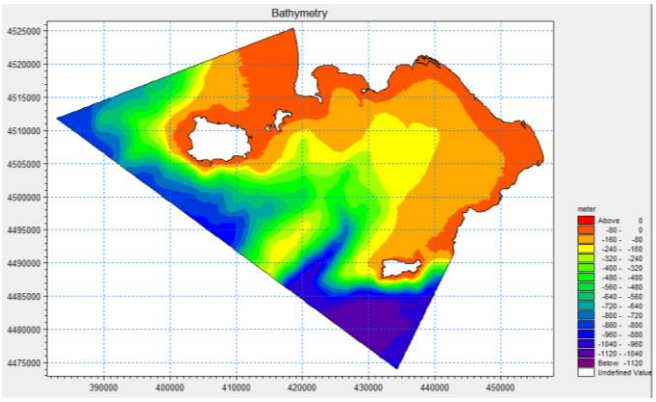

Fig. 4. Zoom of the Gulf of Naples with focus on the computational bathymetry implemented in Mike 21 SW.

For the offshore wave power, which is unaffected by refraction and shoaling, calculations were made based on the 1-hour triple (significant wave height, H_s, mean period, T_m, wave direction, Dir_W) provided by the fictitious WAM model. This approach allowed for the derivation of a 1-hour wave power density and wave energy dataset.

The deep-water expression for irregular waves is:

$$P = \frac{\rho g^2 H_s^2 T_e}{64\pi} \tag{3}$$

where ϱ is the sea water density, g is the gravity acceleration and T_e is the wave energy period.

The energy period in the present study has been assumed as 1.14 T_m. As confirmed for UK [27], Central Brazil [28] and Maldives [29] wave energy assessment, this approach seems more conservative. Equation (4) can be written in the approximate expression:

$$P_{wave} = 0.49\, H_s^2 T_e \tag{4}$$

The nearshore wave power, J_{wave}, corresponding to each nearshore propagated sea state, is determined according to the known relationship:

$$J_{wave} = \frac{1}{16}\rho g H_s^2 C_g \quad (5)$$

where C_g denotes the wave group velocity, expressed as:

$$C_g = \frac{1}{2}\left[1 + \frac{2kh}{sinh(2kh)}\right]\sqrt{\frac{g}{k}tanh(kh)} \quad (6)$$

where k is the wave number and h is the water depth.

E. Statistical methods

This study is motivated by the potential time lag between wind and wave resources. The correlation between wind and wave parameters has been quantified using Pearson's correlation coefficient:

$$r = \frac{1}{N}\sum_{n=1}^{N}\frac{[x(n)-\mu_x][y(n)-\mu_y]}{\sigma_x\sigma_y} \quad (7)$$

where μx, μy, sx, sy are respectively the mean and the standard deviation of the variables x and y, of n observations and N is the total sample size.

The Pearson's coefficient may also be use to give the correspondence between wind and wave, after a certain a time lag τ. In that case, eq. (7) should be rewritten as:

$$C_c = \frac{1}{N}\sum_{n=1}^{N-\tau}\frac{[x(n)-\mu_x][y(n+\tau)-\mu_y]}{\sigma_x\sigma_y} \quad (8)$$

The degree of association between two parameters, x and y, is quantified by the cross-correlation coefficient (C_C). C_C ranges from 0, indicating no correlation, to 1, representing perfect correlation. The time lag at which the correlation reaches its maximum value is considered as the average delay.

To analyse the wind-wave dataset, several multivariate techniques, namely Principal Component Analysis (PCA) and Cluster Analysis (CA), have been employed [30]. PCA and Factor Analysis have been applied to extract eigenvalues and eigenvectors from the covariance matrix of the original variances. The resulting subspace obtained through PCA is expressed as a dense basis with multiple non-zero weights, making interpretation challenging. In order to reduce the impact of less significant parameters within each principal component, a varimax rotation criterion has been applied. The varimax rotation maximizes the sum of the variances of squared correlations between variables and factors, enabling the simplification of the PCA subspace expression by highlighting a few major components. This procedure facilitates the selection of a limited number of components to effectively describe the entire dataset while minimizing the loss of original information.

For analysing the similarities among groups of meteo-climatic data, Cluster Analysis (CA) has been employed. Both hierarchical (HCA) and non-hierarchical K-means methods have been considered for this purpose.

When the analysis focuses on subsets of a few hundred records, hierarchical clustering analysis (HCA) is the preferred approach. However, in cases where several thousand records are being analysed simultaneously, K-means clustering analysis (K-means CA) is more suitable.

In the context of this study, K-means analysis was conducted twice. After the first run, the final cluster centroids obtained were used as initial centres in the second run. Therefore, the results presented in this study pertain to the second run of the K-means analysis.

III. RESULTS

F. Wave and wind power assessment

According to Table I, the average annual wind power density was determined to be 31.52 W/m2 at a height of 10 m. In addition to that, various wind parameters including minimum, maximum, mean, and standard deviation of wind speed, U_V, have been calculated. Fig. 5 illustrates the annual frequency distribution of wind direction, Dir_V, along with the annual mean wind power. The figure clearly demonstrates that the prevailing wind direction is from the West, with a secondary sector originating from the E-NE direction.

Table II presents the nearshore energy density, which is approximately 1.84 kW/m, along with other important parameters. The overall wave climate exhibits average wave parameters, with a significant wave height of 0.39 m, a peak period of 4.9 s, and a mean direction of 199°N. Most of the wave power is contributed by southwest waves, as shown in Fig. 6. The narrow directional sector and the lower-than-expected wave power can be qualitatively explained by considering the specific location of the study point within the Gulf of Naples.

TABLE I
MAIN WIND CLIMATE PARAMETERS AT STUDY SITE

	U_V (m/s)	Dir_V (°)	P_{wind} [W/m]
Mean	3.24	170.38	31.52
Median	2.83	171.43	8.32
Minimum	0.01	0.00	0.00
Maximum	17.36	360.00	1923.25
Std. Deviation	2.07	104.03	67.16
N	368184	368184	368184

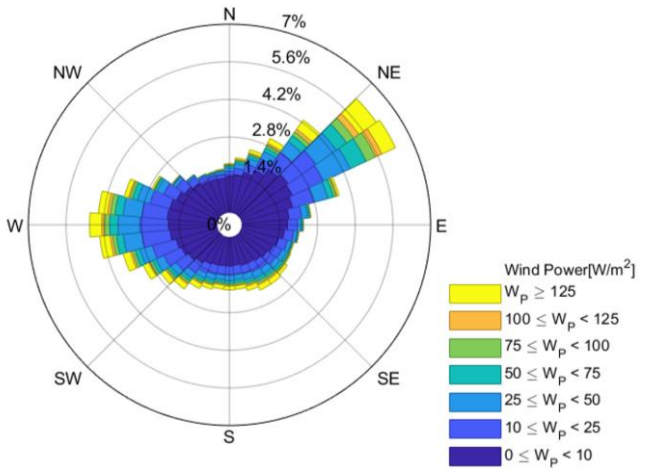

Fig. 5. Characterization of the yearly average wind energy in terms of annual power per meter of wave front (in kWh/m).

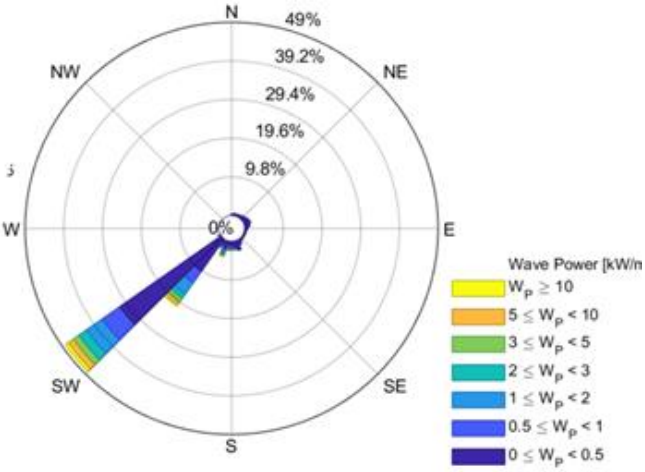

Fig. 6. Characterization of the yearly average wave energy in terms of annual power per meter of wave front (in kWh/m).

G. *Wave and wind correlation*

The correlations among parameters were investigated and reported in Table III. Wind and waves temporal patterns (i.e. annual and monthly) are generally well correlated. However, especially during the period from June to October, there might be conditions for a smaller correlation. These conditions are the most interesting in the perspective of reducing the overall variability of the produced power. Moreover, it is during those months which the floating wind turbine prototype is expected to be investigate. So, its energy will be combined with the power production from OBREC.

In order to identify those patterns, the different meteo-climatic conditions were analyzed by using a PCA/FA and then classified by means of K-means CA. PCA/FA was applied to the wind velocity and direction, wave direction, Tp and Hs. The resulting three components explains 85.83% of the original variance. The first component explains the 40.0% of the whole variance, while 30.2% and 15.6% of the variance is explained, respectively by the second and the third component. The factor loadings of the PCA/FA solution are shown in Table IV. The factor selection was evaluated on the basis of the scree plot (see Figure 7). The first component accounts for just Hs and Tp. The second component accounts for wave direction and wind speed.

The third component accounts for both the wind and wave directions. It is worth to note that, as in other study on the wave-wind correlation in the Italian seas [e.g. 11], the first component generally accounts for Hs, Tp and wind speed. This aspect could be attributable to the effect of the coastline proximity, firstly analysed by the present work.

The meaning of these components is better clarified in the K-means CA, which was then applied to the factor scores obtained by the PCA/FA extraction. A five K-means clusters solution was chosen (fig. 8). In Table V the different meteo-climatic characteristics of the five k-means clusters solution are reported. The main characteristics can be summarised as follow:

- K-means cluster 1 shows all the components below the average. It refers to calm meteo-climatic conditions in which waves are coming from southwest and winds are blowing from East.
- K-means cluster 2 refers to the most energetic sea states in the subset. A significant wind blows with very similar direction to nearshore waves.
- K-means cluster 3 highlights poor wave conditions associated to strong wind events. Both wave and wind direction are related to East-Southeast sector.
- K-means cluster 4 is characterized by intense wave conditions. Weak winds from East below blow in opposite direction to waves;
- K-means cluster 5 highlights the condition for which small waves and wind come from the same direction (W-SW).

TABLE II
MAIN WAVE CLIMATE PARAMETERS AT STUDY SITE

	$H_{s,mean}$ (m)	$T_{m,\ mean}$ (s)	Dir_w (°)	J_{wave} [kW/m]
Mean	0.39	4.92	199.13	1.84
Median	0.26	4.81	224.85	0.26
Minimum	0.01	1.81	0.01	0.00
Maximum	4.93	12.11	236.18	325.17
Std. Deviation	0.37	1.69	54.11	5.96

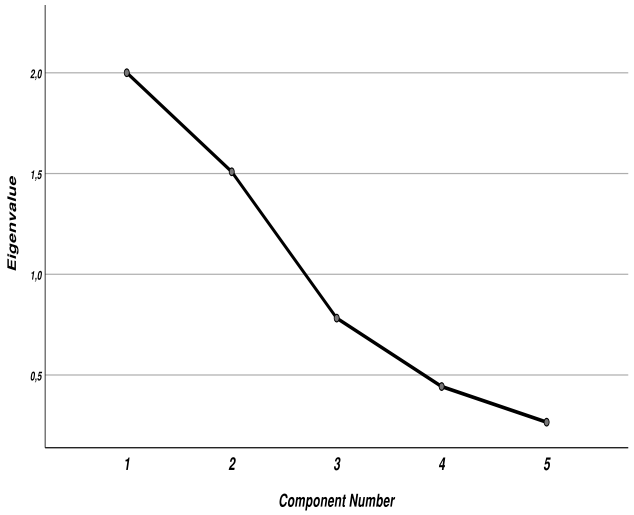

Fig. 7. Scree plot showing the extracted components and their corresponding eigenvalues. Three components present eigenvalue higher than or 0.75. Only these were considered in the analysis.

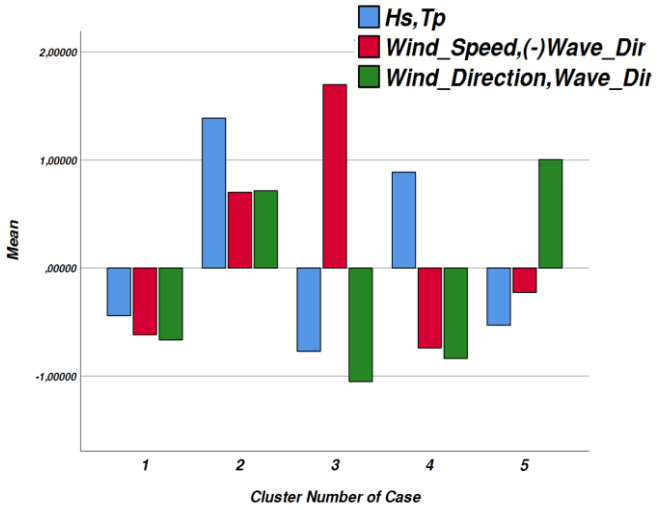

Fig. 8. Standardized characteristics of the five K-means clusters (e.g. zero corresponds to the sample average, while the sample standard deviation is 1).

The comparison of the wave-wind correlations, obtained from the pooled data set (table III) with the correlations obtained after splitting the dataset into the described meteo-climatic clusters (table V), make possible to draw some preliminary considerations. First of all, the clusters showing the lowest correlation between wind speed and significant wave heights are the K-means cluster 1, 3 and 5, with the last two being more interesting in terms of main wind speed: these clusters refer the meteo-climatic conditions that should be dominant to maximize the advantage to combine wind and wave. Furthermore, it is interesting to note as just cluster 3 and 5 show a high correlation in terms of wind-wave directions, albeit with different sign. In the K-means 3, wave and wind forcing are related to "sirocco" (the ancient name of Mediterranean wind coming from SE) meteo-climatic conditions; instead, a clear "libeccio" (the wind from SW) pattern characterize the K-means 5. This aspect, along with the consideration about the first component composition, represent a clear consequence of the proximity of the study site with the shore.

TABLE III
CORRELATIONS MATRIX OF SIGNIFICANT WAVE HEIGHT, H_s (M), WAVE PERIOD T_P (S), MEAN WAVE DIRECTION, DIR_W (°), WIND SPEED, U_V (M/S), MEAN WIND DIRECTION, DIR_V (°).

		H_s	T_p	Dir_w	U_v	Dir_v
H_s	Pearson Correlation	1	.669*	.271*	.406*	.194*
	Sig. (2-tailed)		0.000	0.000	0.000	0.000
	Number of data	368184	368184	368184	368184	368184
T_p	Pearson Correlation	.669*	1	.172*	.273*	.056*
	Sig. (2-tailed)	0.000		0.000	0.000	0.000
	Number of data	368184	368184	368184	368184	368184
Dir_w	Pearson Correlation	.271*	.172*	1	-.295*	.397*
	Sig. (2-tailed)	0.000	0.000		0.000	0.000
	Number of data	368184	368184	368184	368184	368184
U_v	Pearson Correlation	.406*	.273*	-.295*	1	-.055*
	Sig. (2-tailed)	0.000	0.000	0.000		0.000
	Number of data	368184	368184	368184	368184	368184
Dir_v	Pearson Correlation	.194*	.056*	.397*	-.055*	1
	Sig. (2-tailed)	0.000	0.000	0.000	0.000	
	Number of data	368184	368184	368184	368184	368184

*. Correlation is significant at the 0.01 level (2-tailed).

TABLE IV
FACTOR LOADINGS OF THE PCA SOLUTIONS. ONLY HIGHER CORRELATIONS ARE REPORTED.

	Component		
	1	**2**	**3**
Hs	0.884		
Tp	0.906		
Dir_w		-0.696	0.458
U_v		0.861	
Dir_v			0.965

In order to highlight the monthly and interannual occurrence of such conditions, a K-means CA was further applied to the factor scores obtained by the PCA/FA extraction at the time scale of year-month. Figure 8 show the seasonality analysis of each cluster. In doing this kind of analysis, two subsets were identified: Land breeze

dataset (LBD hereinafter), for wind blowing in the range 305-135°N, and Sea-wind dataset (SWD), for wind coming from 135°N to 305°N.

In the case of SWD (Fig. 9a), cluster 1 occurs expecially in September, October and December. Meteo-climatic conditions referred by cluster 3 occurs in all seasons. Finally, events of cluster 5 occour typically in summer. For LBD (fig. 9b), the first three clusters refer to winter events, while cluster 4 shows higher occurrence form May to October and cluster 5 spread in all season, with an hotspot in June and July.

It is worth emphasizing that all K-means clusters, which indicate uncorrelated patterns, are primarily characterized by mild swell conditions, except for cluster 3 in SWD. Therefore, the analysis presented here holds significance for general considerations, even though it has minimal impact on the overall energy patterns of the study site (as the significant wave height is too small to be relevant for wave energy production). The interannual variability of K-means clusters is reported in figure 10, in which clusters have been aggregated along a 5-year period: no significant variation can be detected.

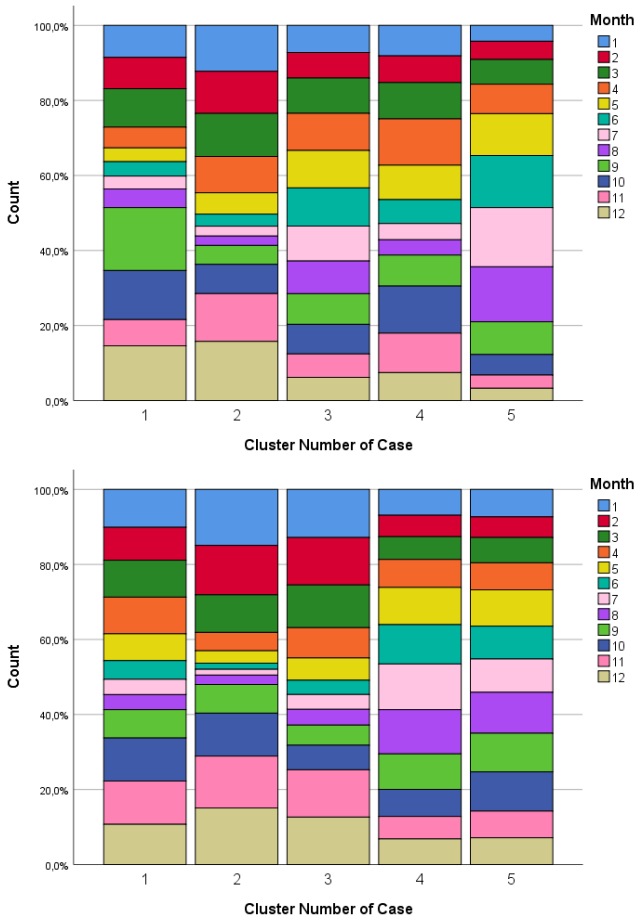

Fig. 9. Bar charts show the monthly distribution of each cluster for: (a) sea breeze subset and (b) land breeze subset.

TABLE V
EXAMPLE VARIABLES AND UNITS FOR MARINE RENEWABLE ENERGY

Cluster Number of Case		H_s	T_p	Dir_w	U_v	Dir_v
1	Mean	0.1971	3.9128	209.6056	2.0338	90.8174
	Median	0.1649	3.8880	225.3108	1.8864	83.3868
	Minimum	0.01	1.81	37.24	0.01	0.00
	Maximum	0.94	8.36	236.18	6.97	309.66
	Std. Deviation	0.13112	1.01576	29.13796	1.13682	55.29555
	N	79374	79374	79374	79374	79374
2	Mean	0.9842	6.7547	218.6601	5.6562	236.0690
	Median	0.8700	6.7030	224.8961	5.3713	247.4191
	Minimum	0.04	3.18	18.24	0.25	4.81
	Maximum	4.93	12.11	236.18	17.36	360.00
	Std. Deviation	0.45926	1.27135	16.09335	2.10678	56.68571
	N	56399	56399	56399	56399	56399
3	Mean	0.1322	4.2578	79.7003	5.1158	68.5518
	Median	0.1209	4.2410	70.9623	4.9164	55.9145
	Minimum	0.01	1.81	0.01	0.05	0.01
	Maximum	0.97	9.89	233.97	15.27	359.99
	Std. Deviation	0.08225	1.08262	47.70617	2.00235	52.51385
	N	49462	49462	49462	49462	49462
4	Mean	0.5470	6.5333	220.5251	2.4298	99.1341
	Median	0.5161	6.2650	225.3251	2.2761	81.1318
	Minimum	0.01	3.25	12.50	0.01	0.00
	Maximum	2.75	11.84	236.18	8.65	358.59
	Std. Deviation	0.26863	1.09531	14.66153	1.28688	69.33839
	N	64699	64699	64699	64699	64699
5	Mean	0.2650	4.1061	221.0598	2.5523	274.0464
	Median	0.2181	3.9560	226.0581	2.4431	275.5026
	Minimum	0.01	1.81	9.11	0.01	97.79
	Maximum	1.13	9.20	236.17	11.56	360.00
	Std. Deviation	0.16572	1.30762	19.97942	1.31962	46.44345
	N	118250	118250	118250	118250	118250
Total	Mean	0.3922	4.9170	199.1386	3.2388	170.3854
	Median	0.2634	4.8140	224.8541	2.8281	171.4345
	Minimum	0.01	1.81	0.01	0.01	0.00
	Maximum	4.93	12.11	236.18	17.36	360.00
	Std. Deviation	0.37257	1.68844	54.10695	2.07250	104.02693
	N	368184	368184	368184	368184	368184

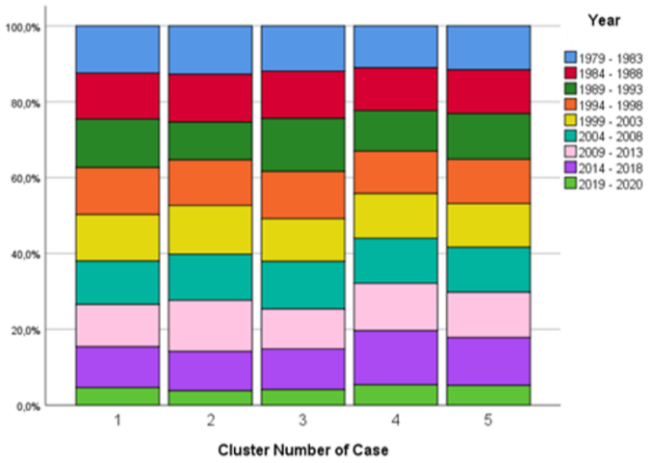

Fig. 10. Frequency of the five wind-wave clusters at the study site, aggregated along a 5-year period.

IV. CONCLUSION

This study investigates the wind speed and sea state patterns at MaRELab, located in the middle of the Mediterranean Sea. The focus is on distinguishing between sea winds and land breezes to analyze their impacts on the wave energy flux in the 25-meter water depth. The unique meteo-climatic conditions of the Tyrrhenian Sea and the nearshore location provide novel findings not previously reported in the literature.

Using a 42-year hourly hindcast dataset (ERA5), the study examines the wind speeds and sea states. The nearshore wave power density is determined to be 1.84 kW/m, and the average annual wind energy flux at a height of 10 meters is estimated at 31.52 W/m2. Sea winds predominantly originate from the west, while land breezes come from the east-northeast. Surprisingly, the occurrence frequencies of both types of local winds are almost equal. Advanced statistical analysis techniques such as Principal Component Analysis (PCA), Factor Analysis (FA), K-means Cluster Analysis (CA), and Hierarchical Cluster Analysis (HCA) are employed to identify dominant meteo-climatic conditions for maximizing the combination of wind and wave energy.

The study reveals higher seasonality in wave energy compared to wind resource. Additionally, an unexpected interannual variability is observed in certain clusters identified by the K-means analysis. Notably, an increase in cluster 1 is observed since 2014, representing calm sea states and uncorrelated winds blowing slightly above the average value of approximately 240°N. This suggests potential climate change effects in the middle Tyrrhenian Sea, requiring further investigation over the coming years.

The low Pearson's correlation coefficients between winds and waves at MaRELab can be explained by the special conditions at the study site, where the narrow wave sector at the entrance of the Gulf of Naples tends to be influenced by local winds, resulting in a delayed impact on the nearshore wave pattern.

The findings of this study contribute to defining design conditions for future wave/wind floating prototypes at MaRELab and can be applied to more energetic sites. Further research is crucial to understanding the complex interaction between local thermal wind and wave patterns at nearshore locations, as well as the implications of their combination on the survival strategies and dynamics of blue energy technologies.

REFERENCES

[1] Palma, G., Contestabile, P., Mizar Formentin, S., Vicinanza, D., & Zanuttigh, B. (2016, November). Design optimization of a multifunctional wave energy device. In Progress in Renewable Energies Offshore, Proceedings of the 2nd International Conference on Renewable Energies Offshore (RENEW2016), Lisbon, Portugal, 24–26 October 2016 (p. 235).

[2] Calheiros-Cabral, T., Clemente, D., Rosa-Santos, P., Taveira-Pinto, F., Ramos, V., Morais, T., & Cestaro, H. (2020). Evaluation of the annual electricity production of a hybrid breakwater-integrated wave energy converter. *Energy*, *213*, 118845.

[3] Di Lauro, E., Maza, M., Lara, J. L., Losada, I. J., Contestabile, P., & Vicinanza, D. (2020). Advantages of an innovative vertical breakwater with an overtopping wave energy converter. Coastal Engineering, 159, 103713.

[4] Vicinanza, D., Lauro, E. D., Contestabile, P., Gisonni, C., Lara, J. L., & Losada, I. J. (2019). Review of innovative harbor breakwaters for wave-energy conversion. *Journal of Waterway, Port, Coastal, and Ocean Engineering*, *145*(4), 03119001.

[5] Naty, S., Viviano, A., & Foti, E. (2016). Wave energy exploitation system integrated in the coastal structure of a Mediterranean port. Sustainability, 8(12), 1342.

[6] Vicinanza, D., Ciardulli, F., Buccino, M., Calabrese, M., & Koefed, J. P. (2011). Wave loadings acting on an innovative breakwater for energy production. Journal of Coastal Research, 608-612.

[7] Contestabile, P., & Vicinanza, D. (2018). Coastal defence integrating wave-energy-based desalination: A case study in Madagascar. Journal of Marine Science and Engineering, 6(2), 64.

[8] Azzellino, A., Ferrante, V., Kofoed, J. P., Lanfredi, C., & Vicinanza, D. (2013). Optimal siting of offshore wind-power combined with wave energy through a marine spatial planning approach. *International Journal of Marine Energy*, *3*, e11-e25.

[9] Jacobsen, H. K., Hevia-Koch, P., & Wolter, C. (2019). Nearshore and offshore wind development: Costs and competitive advantage exemplified by nearshore wind in Denmark. *Energy for Sustainable Development*, *50*, 91-100.

[10] Azzellino, A., Lanfredi, C., Contestabile, P., Ferrante, V., & Vicinanza, D. (2011, June). Strategic environmental assessment to evaluate WEC projects in the perspective of the environmental cost-benefit analysis. In *The Twenty-first International Offshore and Polar Engineering Conference*. OnePetro.

[11] Azzellino, A., Lanfredi, C., Riefolo, L., De Santis, V., Contestabile, P., & Vicinanza, D. (2019). Combined exploitation of offshore wind and wave energy in the Italian seas: a spatial planning approach. *Frontiers in Energy Research*, *7*, 42.

[12] Perez Collazo, C., Astariz, S., Abanades, J., Greaves, D., & Iglesias, G. (2014, October). Co-located wave and offshore wind farms: A preliminary case study of an hybrid array. In *International conference in coastal engineering (ICCE)*.

[13] Seroka, G., Fredj, E., Kohut, J., Dunk, R., Miles, T., & Glenn, S. (2018). Sea breeze sensitivity to coastal upwelling and synoptic flow using Lagrangian methods. *Journal of Geophysical Research: Atmospheres*, *123*(17), 9443-9461.

[14] Contestabile, P., Lauro, E. D., Galli, P., Corselli, C., & Vicinanza, D. (2017). Offshore wind and wave energy assessment around Malè and Magoodhoo Island (Maldives). Sustainability, 9(4), 613

[15] Ferrari, F., Besio, G., Cassola, F., & Mazzino, A. (2020). Optimized wind and wave energy resource assessment and offshore exploitability in the Mediterranean Sea. *Energy*, *190*, 116447.

[16] Diaconu, S., Onea, F., & Rusu, E. (2013). Evaluation of the nearshore impact of a hybrid wave-wind energy farm. *International Journal of Education and Research*, *1*(2), 1-28.

[17] Rodriguez-Delgado, C., Bergillos, R. J., & Iglesias, G. (2019). Dual wave farms and coastline dynamics: The role of inter-device spacing. *Science of The Total Environment*, *646*, 1241-1252.

[18] Contestabile, P., Ferrante, V., Di Lauro, E., & Vicinanza, D. (2017). Full-scale prototype of an overtopping breakwater for wave energy conversion. Coastal Engineering Proceedings, 1(35), 12.

[19] Contestabile, P., Crispino, G., Russo, S., Gisonni, C., Cascetta, F., & Vicinanza, D. (2020). Crown wall modifications as response to wave overtopping under a future sea level scenario: An experimental parametric study for an innovative composite seawall. Applied Sciences, A10(7), 2227.

[20] Contestabile, P., Crispino, G., Di Lauro, E., Ferrante, V., Gisonni, C., & Vicinanza, D. (2020). Overtopping breakwater for wave Energy Conversion: Review of state of art, recent advancements and what lies ahead. *Renewable Energy*, *147*, 705-718.

[21] Palma, G., Contestabile, P., Zanuttigh, B., Formentin, S. M., & Vicinanza, D. (2020). Integrated assessment of the hydraulic and structural performance of the OBREC device in the Gulf of Naples, Italy. *Applied Ocean Research*, *101*, 102217.

[22] Contestabile, P., Russo, S., Azzellino, A., Cascetta, F., & Vicinanza, D. (2022). Combination of local sea winds/land breezes and nearshore wave energy resource: Case study at MaRELab (Naples, Italy). *Energy Conversion and Management*, *257*, 115356.

[23] European Centre for Medium-Range Weather Forecasts (ECMWF). May 2023 [Online] Available: https://climate.copernicus.eu/climate-reanalysis.

[24] DHI Water and Environment. May 2023 [Online] Available: https://www.mikepoweredbydhi.com/download/mike-2017-sp2/mike-21?ref=%7B40160C10-5509-4460-A36F-FA2759EAC02F%7D

[25] Contestabile, P., Conversano, F., Centurioni, L., Golia, U. M., Musco, L., Danovaro, R., & Vicinanza, D. (2020). Multi-collocation-based estimation of wave climate in a non-tidal bay: The case study of Bagnoli-Coroglio bay (Tyrrhenian Sea). Water, 12(7), 1936.

[26] General Bathymetric Chart of the Oceans. May 2023 [Online] Available: http://www.gebco.net/

[27] ABP Marine Environmental Research Ltd. Atlas of UK Marine Renewable Energy Resources: Technical Report; Report No. R.1106 Prepared for the UK Department of Trade and Industry; ABP Marine Environmental Research Ltd.: Southampton, UK, 2004.

[28] Contestabile, P., Ferrante, V., & Vicinanza, D. (2015). Wave energy resource along the coast of Santa Catarina (Brazil). *Energies*, *8*(12), 14219-14243.

[29] Contestabile, P., Di Lauro, E., Galli, P., Corselli, C., & Vicinanza, D. (2017). Offshore wind and wave energy assessment around Malè and Magoodhoo Island (Maldives). *Sustainability*, *9*(4), 613.

[30] A. Afifi, V. Clark, in: Computer-Aided Multivariate Analysis, fourth ed., Texts in Statistical Science, Chapman & Hall/CRC Press, 1996.